and short-chained chelated hemes, but at a significantly higher frequency, 507 cm^{-1}, for the 2-methylimidazole-chelated heme. Essentially the same frequency, 506 cm^{-1}, is observed for the CO adduct of the 1,2-dimethylimidazole complex of mesoheme dimethyl ester (bottom spectrum). An upshift in the Fe–CO frequency has previously been noted by Yu and co-workers, when the trans-axial ligand is sterically hindered or has a weak field (e.g. tetrahydrofuran).[36] Evidently the Fe–CO bond is strengthened as the bond to the trans ligand is weakened, in contrast to the situation with O_2 adducts, where a small effect in the opposite direction has been observed.[37] We note, however, the recent controversy over the ν_{Fe-O_2} assignment.[38]

The remaining bands in the low-frequency region have been tentatively assigned to both in-plane and out-of-plane porphyrin deformation modes.[39,40] We note that a new band appears, at 158 cm^{-1}, both for the 1,2-Me_2Im mesoheme dimethyl ester adduct and for the 2-methylimidazole-chelated heme. This may be an additional out-of-plane mode, activated by the nonbonded influence of the 2-methyl group, or it may be a mode of the ligand itself, coupled to the porphyrin electronic system via the 2-methyl interaction. A band at 157 cm^{-1} is seen for deoxyhemoglobin[22,32,41] but has not been assigned.

D. Steric Effects and CO Binding. CO dissociation rates have been measured[2-4] for the chelated hemes included in this study. Although the short-chained chelated heme, **2**, is suggested by CPK models to be somewhat strained, the CO off-rate is increased relative to **1** only by a modest factor of 2.[3] We see no evidence for strain in our spectroscopic measurements. All of the RR frequencies are the same for the two chelated hemes, in both ligated and unligated forms. In particular, the Fe–Im stretching frequency in the unligated form and the Fe–CO frequency in the CO adduct are the same.

Addition of a methyl group at the imidazole C2 position, however, produces a dramatic effect, both in the CO off-rate, which is increased by over a factor of 10,[3] and in the RR spectra. It has previously been emphasized[3] that the 2-methyl group has an even larger steric effect on the chelated heme than in the absence of chelation, since the H atom it replaces is inside the chelate ring. Consistent with this view is the large decrease in the Fe–Im frequency in the unligated state, even relative to that of the 1,2-dimethylimidazole adduct of mesoheme (178 vs. 194 cm^{-1}). Thus, the Fe–Im bond appears to be substantially weakened by the steric strain introduced by the 2-methyl group in the chelated heme (vida supra). For the CO adduct of **3** the Fe–CO frequency is increased as expected for hindered imidazoles,[36] although by no more than in the 1,2-Me_2Im adduct of mesoheme dimethyl ester. Thus, the enhanced CO dissociation rate is not associated with any weakening in the Fe–CO bond (it is actually somewhat stronger than in the other chelated heme adducts). We suggest that the force responsible for the enhanced off-rate is stored in an expansion of the porphyrin ring, as implied by the lowered ν_3 frequency (1494 vs. 1500 cm^{-1}), brought about by the enhanced steric strain generated by formation of the low-spin CO adduct. Release of the CO would relieve this augmented steric strain.

Acknowledgment. This work was supported by NIH Grants GM 33516 (to T.G.S.) and HL 13581 (to T.G.T.).

(36) Kerr, E. A.; Mackin, H. C.; and Yu, N.-T. *Biochemistry* **1983**, *22*, 4373.
(37) Walters, M. A.; Spiro, T. G.; Suslick, K. S.; Collman, J. P. *J. Am. Chem. Soc.* **1980**, *102*, 6857.
(38) Benko, B.; Yu, N.-T. *Proc. Natl. Acad. Sci. U.S.A.* **1983**, *80*, 7042.
(39) Choi, S.; Spiro, T. G. *J. Am. Chem. Soc.* **1983**, *105*, 3683.
(40) Mitchell, M. L.; Li, X.-Y.; Kincaid, J. R.; Spiro, T. G., manuscript in preparation.
(41) Ondrias, M. R.; Rousseau, D. L.; Simon, S. R. *J. Biol. Chem.* **1983**, *258*, 5638.

Contribution from the Department of Chemistry, University of California, Riverside, California 92521

Redox Chemistry for the Mononuclear Tris(picolinato)-, Tris(acetylacetonato)-, and Tris(8-quinolinato)manganese(III) Complexes: Reaction Mimics for the Water-Oxidation Cofactor in Photosystem II

KENNETH YAMAGUCHI and DONALD T. SAWYER*

Received September 5, 1984

The water-oxidation process ($2H_2O \rightarrow O_2 + 4H^+ + 4e^-$; $E°'$(pH 7) = +0.82 V vs. NHE) of green plant photosynthesis apparently makes use of a multinuclear manganese catalytic center. With the goal to model this process in terms of the requisite redox thermodynamics, ligand stability, and biologically relevant donor groups, a series of manganese(III) complexes ($Mn^{III}L_3$; L = 8-quinolinate, acetylacetonate, picolinate, 2,6-pyridinedicarboxylic acid) have been synthesized. The oxidation–reduction processes for each of these complexes have been characterized in aprotic media by cyclic voltammetry, UV–visible spectroscopy, and magnetic measurements. In the case of the picolinate and acetylacetonate complexes, electrochemical oxidation yields a transiently stable $Mn^{IV}L_3^+$ species that rapidly oxidizes H_2O_2 and OH^-. The redox thermodynamics for the Mn(III)/Mn(IV) and Mn(III)/Mn(II) couples for this group of $Mn^{III}L_3$ complexes and their hydrolytic derivatives are discussed in relation to the water-oxidation process of photosystem II.

Manganese is believed to be an essential electron-transfer agent in the charge accumulation center of the water-oxidizing system of photosystem II (PS II) in green plants.[1-4] Its probable role is as a template to bring the oxygen atoms of two water molecules into close proximity to form an O–O bond. In the chloroplasts of green plants there is a loosely bound pool of manganese that acts as a multicentered catalyst for the oxidation of water to dioxygen. However, the number of manganese ions, their oxidation states, and their structural environments are not known.

Flash-photolysis techniques[5-8] produce reactive intermediates of the oxygen evolution center of the chloroplasts (photosystem II). NMR relaxation experiments indicate that during the cyclic process photooxidation of Mn(II) to Mn(III) occurs and that the resting dark-adapted state involves a mixed oxidation state multinuclear manganese complex. In 1970 a four-state mechanism for the photosystem II oxygen-evolution reaction was proposed.[9]

(1) Heath, R L. *Int. Rev. Cytol.* **1973**, *34*, 49.
(2) Lawrence, G. L.; Sawyer, D. T. *Coord. Chem. Rev.* **1978**, *27*, 173.
(3) Yamaguchi, K. S.; Sawyer, D. T. *Isr. J. Chem.*, in press.
(4) Sauer, K. *Acc. Chem. Res.* **1980**, *13*, 249.
(5) Joliot, P. *Photochem. Photobiol.* **1968**, *8*, 451.
(6) Joliot, P. *Biochim. Biophys. Acta* **1965**, *102*, 116.
(7) Joliot, P.; Barbieri, G.; Chaubaud, R. *Photochem. Photobiol.* **1969**, *10*, 309.
(8) Joliot, P.; Joliot, A. *Biochim. Biophys. Acta* **1968**, *153*, 625.
(9) Kok, B.; Forbush, B.; McGloin, M. *Photochem. Photobiol.* **1970**, *11*, 457.

0020-1669/85/1324-0971$01.50/0

These considerations, as well as the four-electron stoichiometry for the formation of an O_2 molecule from two H_2O molecules, indicate that between two and four manganese atoms probably are involved per water-oxidizing unit. A recent report[10] describes the isolation of a 34-kDa protein that contains two manganese ions (apparently in the Mn(III) oxidation state). Independent of the number of manganese ions, if they are the redox catalyst for the water-oxidation reaction, then higher valent forms of manganese are involved in the catalytic cycle. Evidence for a Mn(III) → Mn(IV) transition in isolated chloroplasts has been presented.[11]

The proposed role of manganese in the buildup of oxidizing power has been based on the availability of higher oxidation states and variable coordination numbers.[12,13] In order to understand the role of the manganese cofactor in biological electron-transfer reactions, studies of manganese complexes that mimic its reaction chemistry are needed. The redox chemistry of manganese(III) and -(IV) coordination complexes has been summarized in a recent review.[3]

A requisite criterion for the design of model manganese systems for the water-oxidation reaction in PS II is that they must have a sufficiently positive potential to oxidize water (at least +0.82 V vs. NHE at pH 7). The present paper summarizes the results of electrochemical, spectrophotometric, and magnetic studies of a series of mononuclear manganese(III) complexes that are formed by picolinic acid, acetylacetone, 8-quinolinol, 2,6-pyridinedicarboxylic acid, and 2,2′-bipyridine ligands.

Experimental Section

Equipment. A three-electron potentiostat (Princeton Applied Research Model 173 potentiostat/galvanostat with Model 175 universal programmer and Model 179 digital coulometer or a Bioanalytical Systems Model CV-1B) was used for the cyclic voltammetric and controlled-potential electrolysis experiments, and the voltammetric experiments were conducted in Brinkman electrochemical cells. Some of the controlled-potential electrolysis syntheses made use of a Bioanalytical Systems Model SP-2 potentiostat. The cyclic voltammograms were recorded on a Houston Instrument Series 200 recorder.

The controlled-potential electrolysis experiments made use of a double-fritted H-cell with a center compartment to provide protection from contamination by electrolysis products of the auxiliary electrode (it had provision for replacement of the supporting electrolyte solutions). The working electrodes were a Beckman platinum inlay (area 0.23 cm^2), a Bioanalytical Systems platinum inlay (area 0.023 cm^2), and a Bioanalytical glassy-carbon inlay (area 0.11 cm^2). The controlled-potential electrolysis experiments make use of a platinum-mesh working electrode or sheets of graphitized carbon. The electrochemical systems used a platinum-mesh auxiliary electrode and an Ag/AgCl reference electrode that was filled with an aqueous tetramethylammonium chloride solution and adjusted to 0.00 V vs. SCE.[14] The latter was contained in a Pyrex tube with a soft-glass cracked tip, and this electrode was placed inside a luggin capillary. The platinum-mesh auxiliary electrode was placed inside a glass compartment that was closed with a medium-porosity glass frit. For the controlled-potential experiments the auxiliary electrode was placed in a separate compartment in the double-fritted H-cell. Activated alumina was added to trap protons produced in the auxiliary compartment.

Cary Model 17D and Model 219 spectrophotometers were used for UV-visible spectrophotometric measurements. Low-temperature electronic spectra were measured with a specially constructed Dewar with quartz optical windows (an acetonitrile–dry ice slurry (−21.0 °C) was used as the heat sink). Sample solutions were placed in a 2-mm thick quartz cell and immersed in the acetonitrile–dry ice bath.

The ESR spectra were obtained with a Bruker Model 200R X-band spectrometer equipped with an Oxford Instruments liquid-helium cryostat and temperature controller for low-temperature measurements. The solution magnetic susceptibility measurements were made with a Varian EM-390 NMR spectrometer by the method of Evans[15] as modified by Rettig[16] and made use of the paramagnetic shift of the methyl protons of Me_2SO or MeCN or of Me_4Si (added as an internal standard). Low-temperature solution magnetic moments were measured by use of JEOL 200-MHz or Nicolet 300-MHz NMR spectrometer equipped with liquid-nitrogen purge lines. Pascal constants were used for diamagnetic corrections.[17] Solid-state magnetic moments were measured with a Gouy balance and with a variable-temperature super-conducting susceptometer/magnetometer system, Model 405 (SQUID).

Reagents. The reagents for the investigations and syntheses included $Mn^{II}(ClO_4)_2 \cdot 6H_2O$ (G. Frederick Smith), $Mn^{II}(ClO_4)_2 \cdot H_2O$ (Mallinckrodt), $Mn^{III}(OAc)_3 \cdot 2H_2O$ (Aldrich), 8-quinolinol (Mallinckrodt), picolinic acid (Aldrich), 2,4-pentanedione (Aldrich), 2,6-pyridinedicarboxylic acid (Aldrich), 2,2′-bipyridine (Aldrich), tetraethylammonium hydroxide ((TEA)OH) (25% in water; Aldrich), and tetraethylammonium perchlorate (TEAP) (G. Frederick Smith). The following solvents for all of the experiments were "distilled in glass" grade from Burdick and Jackson and were used without further purification: dimethyl sulfoxide (Me_2SO), acetonitrile (MeCN), dimethylformamide (DMF), and pyridine. High-purity argon gas was used to deaerate the solutions. The elemental analyses were provided by Galbraith Laboratories; some of the manganese assays for the isolated complexes were accomplished by voltammetry measurements.

Preparation of Complexes. Several manganese(II) and -(III) complexes were prepared by conventional methods: $Mn^{III}(acac)_3$ (Hacac = acetylacetone),[18] $[Mn^{III}(urea)_6](ClO_4)_3$,[19] $Mn^{III}(8\text{-}Q)_3$ (8-QH = 8-quinolinol),[20,21] $pyH[Mn^{III}(DPA)_2]$ ($DPAH_2$ = 2,6-pyridinedicarboxylic acid, py = pyridine),[20] $Mn^{III}(PA)_3(H_2O)$, (PAH = picolinic acid),[20,21] $Mn^{III}(DPA)(DPAH)(EtOH)$,[20] $[Mn^{III}(Me_2SO)_6](ClO_4)_3$,[22] $[Mn^{III}(DMF)_6](ClO_4)_3$.[22] The remainder of the complexes were prepared by new synthetic procedures.

$Mn^{III}(PA)_3(H_2O)$. The previous syntheses[20,21] for this complex were modified to obtain a purer product in higher yield. To 2.76 g (2.24×10^{-2} mol) of picolinic acid (PAH) in 40 mL of hot MeCN was added 2.0 g (7.46×10^{-3} mol) of $Mn^{III}(OAc)_3 \cdot 2H_2O$ (dissolved in 25 mL of hot MeCN). As the solution cooled, a brick red precipitate formed, which was filtered, washed with several cold portions of MeCN, and dried in vacuo over P_2O_5. Anal. Calcd for $MnC_{18}H_{14}N_3O_7$: C, 49.12; H, 3.19; O, 25.50; N, 9.56; Mn, 12.52. Found: C, 48.87; H, 3.39; O, 24.42; N, 9.45; Mn, 12.59. Infrared bands (Nujol mull): 1720 (m), 1698 (s), 1480 (m), 1020 (m), 862 (s), 481 (m) cm^{-1}.

$[Mn^{III}(PA)_2(H_2O)_2]ClO_4$. To 50 mL of MeCN at 0 °C was added 1.5 g (3.41×10^{-3} mol) of $Mn^{III}(PA)_3(H_2O)$, followed by the slow addition of 0.6 mL (6.83×10^{-3} mol) of 70% $HClO_4$. The solid was filtered and washed with several small portions of MeCN and dried in vacuo for 24 h. The dried solid was redissolved in 15 mL of ice cold MeCN, and 0.5 equiv of $HClO_4$ was added dropwise. The light brown precipitate that formed was filtered and washed with several cold portions of MeCN and dried in vacuo over P_2O_5. Anal. Calcd for $MnC_{12}H_{12}N_2O_{10}Cl$: C, 33.13; H, 2.76; O, 36.81; N, 6.44; Cl, 8.16; Mn, 12.7. Found: C, 33.30; H, 2.84; O, 36.58; N, 6.55: Cl, 7.92; Mn, 10.7.

$Na[Mn^{III}(DPA)_2]$. To 1.5 g (3.2 mmol) of $pyH[Mn^{III}(DPA)_2]$ dissolved in a minimal amount of hot absolute ethanol was added 0.129 g (3.2 mmol) of solid NaOH. After the solution was cooled, the resulting precipitate was filtered and washed with cold portions of absolute ethanol and dried in vacuo for 24 h. The dried purple solid was recrystallized from 25 mL of hot MeCN and dried in vacuo over P_2O_5. Anal. Calcd for $NaMnC_{13}H_6O_8N_2$: Na, 5.63; C, 41.16; H, 1.47; O, 31.36; N, 6.86. Found: Na, 5.31; C, 40.67; H, 2.36; O, 32.02; N, 6.43.

$TEA[Mn^{III}(DPA)_2]$. To a solution that contained 4.65 g (0.01 mol) of $pyH[Mn^{III}(DPA)_2]$ dissolved in 30 mL of hot MeCN was added 1.41 mL (0.01 mol) of 20% (TEA)OH. A reddish purple solid formed upon cooling, which was filtered, washed with several portions of cold MeCN, and dried in vacuo over P_2O_5. Anal. Calcd for $MnC_{22}H_{26}N_3O_8$: C, 51.24; H, 5.05; N, 8.16; O 24.85; Mn, 10.7. Found: C, 48.59; H, 5.07; N, 8.42; O, 25.33; Mn, 10.5.

$Mn^{III}(acac)(PA)_2$. To 3.55 g (0.01 mol) of $Mn^{III}(acac)_3$ dissolved in 25 mL of hot MeCN was added 1.23 g (0.01 mol) of picolinic acid

(10) Abramowicz, D.; Raab, T.; Dismukes, C. *Adv. Photosynth. Res., Proc. Int. Congr. Photosynth, 6th* **1984**, *1*, 349.
(11) Dekker, J.; Van Gorkom, H.; Martin, B.; Luberthus, O., *Biochim. Biophys. Acta* **1984**, *764*, 301.
(12) Cheniae, G. *Ann. Rev. Plant Physiol.* **1970**, *168*, 438.
(13) Earley, J. E. *Inorg. Nucl. Chem. Lett.* **1973**, *9*, 487.
(14) Sawyer, D. T.; Roberts, J. L., Jr. "Experimental Electrochemistry for Chemists"; Wiley-interscience: New York, 1974; p 144.
(15) Evans, D. F. *J. Chem. Soc.* **1959**, 2003.
(16) Rettig, M. F., private communication, University of California, Riverside, CA.
(17) Figgis, B. N.; Lewis, J. "Modern Coordination Chemistry"; Lewis, J., Wilkins, R. G., Eds.; Interscience: New York, 1960.
(18) Berg, W.; Truemper, T. J. *J. Phys. Chem.* **1960**, *64*, 487.
(19) Aghabozorg, H.; Palenik, G. J.; Staufer, R. C.; Summers, J. *Inorg. Chem.* **1982**, *21*, 3903.
(20) Summers, J. Ph.D. Dissertation, University of Michigan, 1968; available from University Microfilms International, Ann Arbor, MI.
(21) Ray, M. M.; Adhya, J. N.; Biswas, D.; Poddar, S. N. *Aust. J. Chem.* **1966**, *19*, 1737.
(22) Prabhakaran, C. P.; Patel, C. C. *J. Inorg. Nucl. Chem.* **1968**, *30*, 867.

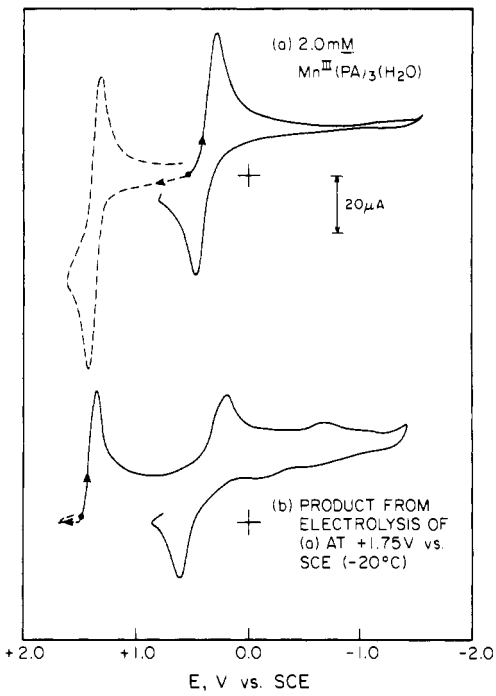

Figure 1. Cyclic voltammograms for 2 mM solutions of (a) $Mn^{III}(PA)_3(H_2O)$ and (b) its oxidation product from electrolysis at +1.75 V vs. SCE (−20 °C) in MeCN (0.1 M tetraethylammonium perchlorate). Conditions: scan rate 0.1 V s^{-1}; indicator electrode, platinum disk (0.23 cm^2); saturated calomel electrode (SCE) vs. NHE, +0.244 V.

dissolved in 30 mL of hot MeCN. The reddish brown precipitate that formed was filtered, washed with cold portions of MeCN, and dried in vacuo over P_2O_5. Anal. Calcd for $MnC_{17}H_{15}O_6N_2$: Mn, 13.81; C, 51.26, H, 3.77; O, 24.12. Found: Mn, 13.61; C, 51.18; H, 4.20; O, 23.76.

$Mn^{III}(acac)(8\text{-}Q)_2$. To 3.55 g (0.01 mol) of $Mn^{III}(acac)_3$ in 25 mL of hot MeCN was added 2.90 g (0.02 mol) of 8-quinolinol in 30 mL of hot MeCN. The dark green solid that formed was filtered, washed with several portions of cold MeCN, and dried in vacuo over P_2O_5. Anal. Calcd for $MnC_{23}H_{19}O_4N_2$: C, 62.41; H, 4.30; O, 14.47. Found: C, 62.23; H, 4.13; O, 14.41.

$Mn^{III}(DPA)(PA)(H_2O)$. Two grams (5.7 mmol) of $Mn^{III}(acac)_3$ in 40 mL of MeCN was added to 0.95 g (5.7 mmol) of 2,6-pyridinedicarboxylic acid and 0.70 g (5.7 mmol) of picolinic acid in 50 mL of hot MeCN. The pink precipitate that formed was filtered, washed with cold portions of MeCN, and dried in vacuo over P_2O_5. Anal. Calcd for $MnC_{13}H_9O_7N_2$: C, 43.31; H, 2.50; N, 7.77; O, 31.10. Found: C, 43.56; H, 2.86; N, 7.20; O, 30.69.

$[Mn^{III}(DPA)(bpy)(H_2O)](ClO_4)$. To 2.0 g (4.6 mmol) of $Mn^{III}(DPA)(DPAH)(EtOH)$ in 30 mL of hot MeCN was added 0.723 g (4.6 mmol) of 2,2′-bipyridine in 10 mL of hot MeCN. The solution was cooled, and 0.5 g (4.6 mmol) of $NaClO_4$ was added. The reddish purple precipitate that formed was filtered, washed with cold portions of MeCN, and dried in vacuo over P_2O_5. Anal. Calcd for $MnC_{17}H_{13}N_3O_9Cl$: C, 41.32, H, 2.63; N, 8.51; O, 29.17. Found: C, 41.94; H, 2.71; N, 7.92; O, 28.95.

$Mn^{III}(DPA)(DPAH)(H_2O)$. To 2.68 g (0.01 mol) of $Mn^{III}(OAc)_3 \cdot 2H_2O$ in 50 mL of hot MeCN was added 3.34 g (0.02 mol) of 2,6-pyridinedicarboxylic acid. Upon cooling, a purple precipitate formed that was filtered, washed with cold portions of MeCN, and dried in vacuo over P_2O_5. The dried solid was recrystallized twice from 20-mL portions of MeCN and dried in vacuo over P_2O_5. Anal. Calcd for $MnC_{14}H_9O_9N_2$: C, 41.57; H, 2.23; O, 35.63; N, 6.93; Mn, 13.6. Found: C, 42.23; H, 2.16; O, 34.05; N, 7.75; Mn, 13.1.

Results

Electrochemistry. The cyclic voltammogram of the $Mn^{III}(PA)_3(H_2O)$ complex in MeCN is shown in Figure 1a. Controlled-potential reduction of this complex at +0.39 V vs. NHE results in the addition of one electron and causes the rest potential to shift negatively. An initial positive scan of the reduced complex exhibits a reversible oxidation peak at +0.71 V vs. NHE (coupled to a reduction peak at +0.58 V). Addition of 1 equiv of protons to the reduced solution causes the anodic peak to disappear and the appearance of a new cathodic peak at −0.62 V (free picolinic acid has a reduction peak at −0.62 V, which disappears when 1 equiv of base is added). These results are consistent with the formation of $Mn^{II}(PA)_3^-$ from the exhaustively reduced $Mn^{III}(PA)_3(H_2O)$ complex. The $Mn^{III}(PA)_3(H_2O)$ complex can be formed in situ by the addition of 3 equiv of picolinic acid to 1 equiv of $Mn^{III}(OAc)_3 \cdot 2H_2O$ in MeCN [the electrochemistry for this combination is essentially the same as that for the isolated $Mn^{II}(PA)_3(H_2O)$ complex (Figure 1a)]. Addition of 1 equiv of protons to the $Mn^{III}(PA)_3(H_2O)$ complex in MeCN results in a new reduction peak at +0.90 V along with reduction peaks at +0.57 and −0.46 V (due to the reduction of the original complex and bound protonated picolinate ligand (PAH), respectively).

An initial positive scan of the $Mn^{III}(PA)_3(H_2O)$ complex yields a reversible one-electron-oxidation peak at +1.64 V vs. NHE coupled to a reduction peak at +1.57 V in MeCN. After the controlled-potential oxidation at +1.79 V of $Mn^{III}(PA)_3(H_2O)$, a negative voltage scan exhibits reduction peaks at +0.90, +0.57, and −0.51 V. The latter two peaks are due to the Mn^{III}/Mn^{II} redox couple and to free picolinic acid produced during the electrolysis, respectively. The reduction peak at +0.90 V is similar to that produced when 1 equiv of acid is added to an acetonitrile solution that contains the $Mn^{III}(PA)_3(H_2O)$ complex. This same reduction peak also is observed when picolinic acid is added to the $Mn^{III}(urea)_6(ClO_4)_3$ complex (2:1 mole ratio) in MeCN. Hence, this reduction is due to the $Mn^{III}(PA)_2^+$ complex. The formation of the $Mn^{III}(PA)_2(H_2O)_2^+$ complex from the $Mn^{IV}(PA)_3^+$ species in the room-temperature exhaustive oxidation probably occurs via electron transfer from the carboxylate group on one of the picolinate ligands to the manganese(IV) ion and subsequent abstraction of a hydrogen atom from the solvent or supporting electrolyte to form the $Mn^{III}(PA)_2(H_2O)_2^+$ complex and free picolinic acid (PAH). The cyclic voltammogram of the synthesized $Mn^{III}(PA)_2(H_2O)_2ClO_4$ complex in MeCN is essentially the same as that for the product from the electrolytic oxidation of $Mn^{III}(PA)_3(H_2O)$.

Figure 1b illustrates that controlled-potential electrolytic oxidation of $Mn^{III}(PA)_3(H_2O)$ at −21 °C yields a stable $Mn^{IV}(PA)_3^+$ species. The reduction peak at +1.63 V decreases with time, and those at +0.90 and −0.47 V increase. The addition of hydroxide ion to a solution of the $Mn^{IV}(PA)_3^+$ complex results in its slow reduction to the $Mn^{III}(PA)_3$ complex (Figure 2).

Figure 3 illustrates that the redox chemistry for the $Mn^{III}(acac)_3$ and $Mn^{III}(8\text{-}Q)_3$ complexes closely parallels that for $Mn^{III}(PA)_3(H_2O)$. The reduction potentials of the Mn(III)/Mn(II) couple and the oxidation potentials of the Mn(III)/Mn(IV) couple for these and related manganese(III) complexes in MeCN are

Table I. Redox Potentials for 1 mM Manganese(III) Complexes in Acetonitrile (0.1 M Tetraethylammonium Perchlorate)

complex[a]	$E^{\circ\prime}$,[b] V vs. NHE Mn(III) ⇄ Mn(II)	Mn(III) ⇄ Mn(IV)
$[Mn^{II}(MeCN)_4](ClO_4)_2$	>+2.54[c]	
$[Mn^{III}(Me_2SO)_6](ClO_4)_3$	+1.19[d]	
$[Mn^{III}(urea)_6](ClO_4)_3$	+1.11[d]	
$Mn^{III}(PA)_3(H_2O)$	+0.62	+1.61
$TEA[Mn^{III}(DPA)_2]$	+0.58	+1.44
$Mn^{III}(DPA)(DPAH)(EtOH)$[e]	+0.59	+1.57[f]
$Mn^{III}(DPA)(PA)(H_2O)$[e]	+0.58	+1.60[f]
$Mn^{III}(PA)_2(acac)$[e]	+0.41	+1.45
$Mn^{III}(acac)_3$	+0.11	+1.21
$Mn^{III}(8\text{-}Q)_3$	+0.16	+1.18
$Mn^{III}(8\text{-}Q)_2(acac)$	+0.06	+1.03
$[Mn^{III}(DPA)(bpy)(H_2O)]ClO_4$[e]	+0.60	+1.43[f]

[a] Key: PA = picolinate; acac = acetylacetonate; 8-Q = 8-quinolinate; DPA = 2,6-pyridinedicarboxylate; TEA = tetraethylammonium cation; bpy = 2,2′-bipyridine. [b] Potentials represent the mean of the cathodic and anodic peak potentials from cyclic voltammograms (scan rate 0.1 V s^{-1}). [c] Anodic peak potential (scan rate 0.1 V s^{-1}). [d] Cathodic peak potential (scan rate 0.1 V s^{-1}). [e] Solubility less than 0.2 mM. [f] Mn(III)/Mn(IV) redox couple irreversible; anodic peak potential (scan rate 0.1 V s^{-1}).

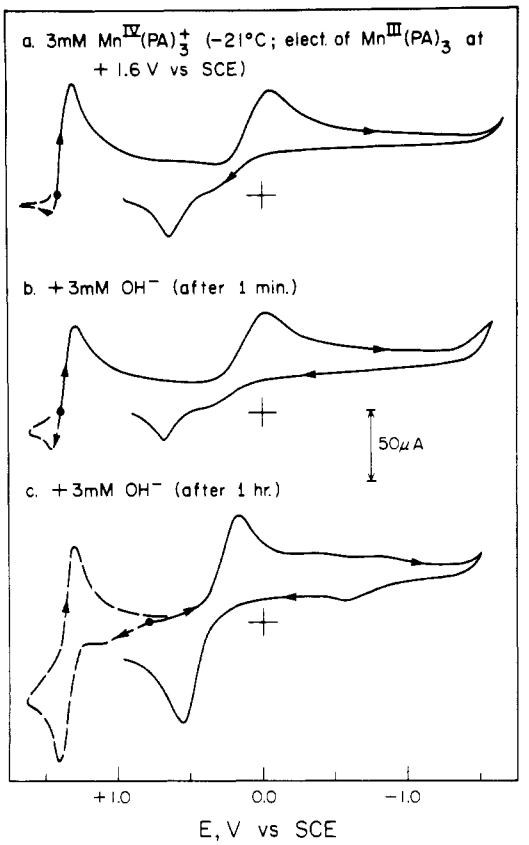

Figure 2. Cyclic voltammograms in MeCN (0.1 M TEAP at −20 °C) of (a) $Mn^{IV}(PA)_3^+$ (from electrolysis of $Mn^{III}(PA)_3$ at +1.75 V), (b) the 1:1 combination of $Mn^{IV}(PA)_3^+$ and OH^- [from tetraethylammonium hydroxide] after 1 min, and (c) solution b after 1 h. Conditions: scan rate 0.1 V s^{-1}; indicator electrode, platinum disk (0.23 cm^2); saturated calomel electrode (SCE) vs. NHE, +0.244 V.

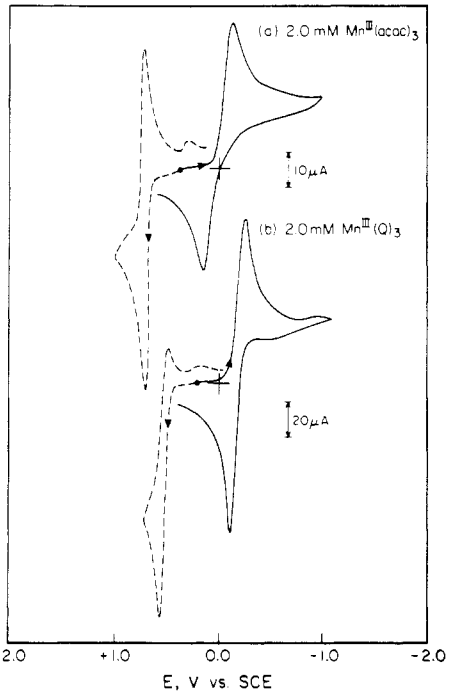

Figure 3. Cyclic voltammograms for 2 mM solutions at (a) $Mn^{III}(acac)_3$ and (b) $Mn^{III}(8\text{-}Q)_3$ in MeCN (0.1 M tetraethylammonium perchlorate). Conditions: potentials referenced relative to the SCE electrode; scan rate 0.1 V s^{-1}; SCE vs. NHE, +0.244 V; indicator electrode, platinum disk (0.23 cm^2).

summarized in Table I. Similar electrochemistry is observed for the complexes in dimethyl sulfoxide solutions, but this solvent is

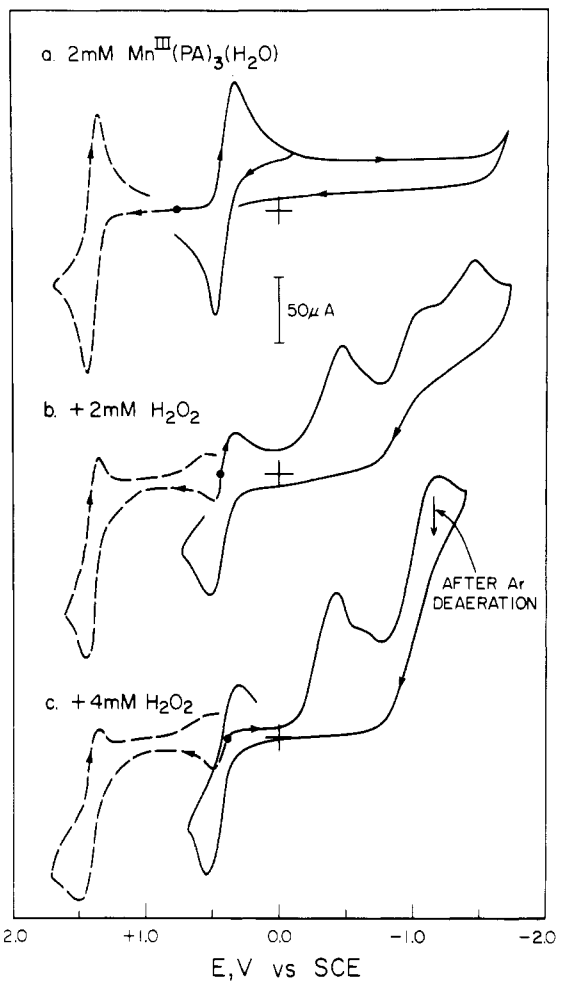

Figure 4. Cyclic voltammograms in MeCN (0.1 M TEAP) of (a) $Mn^{III}(PA)_3(H_2O)$ and (b) a 1:1 and (c) a 1:2 combination of $Mn^{III}(PA)_3(H_2O)$ and H_2O_2. Conditions: scan rate 0.1 V s^{-1}; SCE vs. NHE, +0.244 V; indicator electrode, platinum disk (0.23 cm^2).

oxidized at lower potentials than the Mn(III)/Mn(IV) couple. Controlled-potential electrolysis of $Mn^{III}(acac)_3$ (+1.54 V vs. NHE at −21 °C) yields a stable $Mn^{IV}(acac)_3^+$ species with an initial reduction peak at +1.16 V vs. NHE. The latter decays with time, while the reduction peaks at +0.77 and −1.35 V increase in height. The +0.77-V peak is observed when 1 equiv of acid is added to the $Mn^{III}(acac)_3$ complex in MeCN, and the −1.35-V peak is due to the reduction of free Hacac. These observations indicate that the $Mn^{IV}(acac)_3^+$ complex decomposes to $Mn^{III}(acac)_2^+$ and Hacac. Addition of 1 equiv of base to the exhaustively oxidized solution (−21.0 °C) causes the $Mn^{IV}(acac)_3^+$ species to be reduced to the $Mn^{III}(acac)_3$ complex.

In contrast to the $Mn^{III}(PA)_3(H_2O)$ and $Mn^{III}(acac)_3$ complexes, controlled-potential electrolysis at +1.39 V of the $Mn^{III}(8\text{-}Q)_3$ complex results in the formation of a brown precipitate.

Figure 4 illustrates the cyclic voltammograms that result when H_2O_2 is added to $Mn^{III}(PA)_3(H_2O)$ in MeCN. The reduction peak for the complex is essentially eliminated and replaced with a peak for the reduction of molecular oxygen. this peak disappears when the solution is purged with argon. When 4 mM H_2O_2 is added to a solution that contains 2 mM $Mn^{III}(PA)_3(H_2O)$ and 1.6 mM O_2, the oxygen-reduction peak current increases stoichiometrically. That H_2O_2 oxidized to O_2 by the complex has been confirmed by an evolved-gas manometric experiment.

Spectroscopy. The absorption spectrum for the $Mn^{III}(PA)_3(H_2O)$ complex in MeCN, which is shown in Figure 5, exhibits three peaks. These absorption bands, as well as those of the other manganese(III) complexes in MeCN and Me_2SO solutions, are summarized in Table II. Picolinic acid has an absorbance maximum at 264 nm (ϵ = 3870 M^{-1} cm^{-1}); addition of 1 equiv

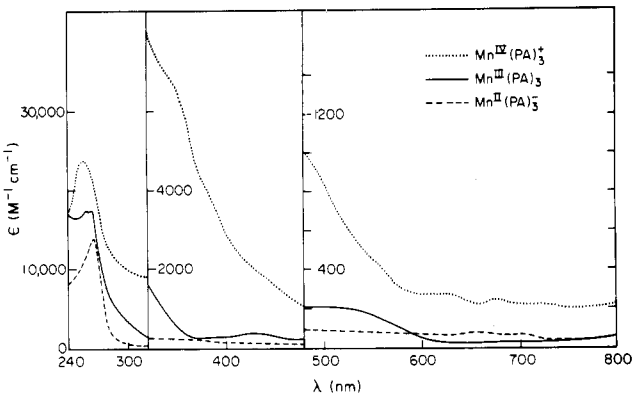

Figure 5. Electronic absorption spectra in MeCN (0.1 M TEAP) of (a) $Mn^{III}(PA)_3(H_2O)$, (b) $Mn^{II}(PA)_3^-$ [from reductive electrolysis at +0.23 V vs. SCE], and (c) $Mn^{IV}(PA)_3^+$ [from oxidative electrolysis at +1.70 V (−21.0 °C)].

Table II. Absorption Spectra for Manganese(III) Complexes and Their Oxidation Products

no.	complex[a]	λ, nm (ε, M^{-1} cm^{-1})
	A. MeCN (0.1 mM)	
1	$[Mn^{III}(Me_2SO)_6](ClO_4)_3$	640 (230), 489 (394), 338 (1708), 270 (1590)
2a	$Mn^{III}(PA)_3(H_2O)$	518 (202), 428 (380), 260 (17 430)
2b	oxidn prod, $[Mn^{IV}]$[b] (electrolysis at +1.7 V)	678 (242), 630 (270), 480 (5042), 348 (6667), 256 (23 781)
3a	$Mn^{III}(acac)_3$	534 (425), 399 (1941), 319 (14 490), 278 (16 491)
3b	oxidn prod, $[Mn^{IV}]$[b]	730 (309), 540 (2130), 388 (5310), 361 (6107), 258 (17 570)
4	$Mn^{III}(PA)_2(acac)$	323 (6620), 264 (14 680)
5	$Mn^{III}Q_3$	482 (672), 393 (11 730), 252 (28 683)
6	$Mn^{III}Q_2(acac)$	388 (7400), 346 (5260), 325 (7520), 254 (53 120)
7	$TEA[Mn^{III}(DPA)_2]$	520 (300), 484 (208), 264 (6720), 230 (11 160)
	B. Me_2SO (5 mM)	
8	$Mn^{III}(DPA)(DPAH)(EtOH)$	590 (193), 498 (340)
9	$Mn^{III}(DPA)(DPAH)(H_2O)$	518 (282)
10	$Mn^{III}(DPA)(PA)(H_2O)$	520 (264), 308 (1720)
11	$[Mn^{III}(DPA)(bpy)(H_2O)]ClO_4$	590 (168), 500 (348)

[a] Key: PA = picolinate; acac = acetylacetonate; 8-Q = 8-quinolinate; bpy = 2,2′-bipyridine; TEA = tetraethylammonium ion. [b] Electrolysis and spectra for solutions at −21 °C.

of base causes the molar absorptivity to decrease to 2505 M^{-1} cm^{-1}.

Controlled-potential electrolytic reduction (at +0.26 V vs. NHE) of the $Mn^{III}(PA)_3(H_2O)$ complex in MeCN causes the visible absorption bands to disappear and the doublets at 263 and 258 nm to shift to 265 nm (Figure 5; Table II). The low-temperature (−21 °C) absorption spectrum for the product from the exhaustive oxidation (at +1.6 V vs. NHE) of the $Mn^{III}(PA)_3(H_2O)$ complex in MeCN also is shown in Figure 5.

Magnetic Moments. The room-temperature magnetic moments for the various magnanese(III) complexes in the solid phase and as 2 mM solutions in Me_2SO are summarized in Table III. For all of the complexes the observed moments are close to the spin-only value of 4.90 μ_B that is expected for mononuclear high-spin six-coordinate d^4 complexes. Variable-temperature (6–320 K) magnetic susceptibility measurements for the solid $Mn^{III}Q_3$, $Mn^{III}(acac)_3$, and $Mn^{III}(PA)_2(H_2O)$ complexes at field strengths of 10 000 and 40 000 G yield linear plots for the reciprocals of corrected molar susceptibilities vs. temperature. This indicates adherence to the Curie-Weiss law for these complexes and that they are mononuclear d^4 systems. Their observed magnetic moments are in the range from 4.7 to 5.0 μ_B.

Table III. Solid and Solution Magnetic Moments for the Manganese(III) Complexes[a]

	μ_{eff}, μ_B	
complex[b]	pure solid[c]	2 mM Me_2SO soln[d]
$Mn^{III}(8\text{-}Q)_3$	4.82[e]	4.90
$Mn^{III}(acac)_3$	4.91	5.10
$Mn^{III}(PA)_3(H_2O)$	4.90, 4.95[e]	4.92
$Mn^{III}(acac)(PA)_2$	4.85	4.99
$Mn^{III}(acac)(Q)_2$	4.84	5.00
$[Mn^{III}(PA)_2(H_2O)_2](ClO_4)$	4.79	4.74
$Mn^{III}(DPA)(DPAH)(H_2O)$	4.98	5.17
$TEA[Mn^{III}(DPA)_2]$	5.08	4.80
$Mn^{III}(DPA)(PA)(H_2O)$	5.10	4.91
$[Mn^{III}(DPA)(bpy)(H_2O)](ClO_4)$	5.27	5.05
$Mn^{III}(DPA)(DPAH)(EtOH)$	4.95, 4.92[e]	5.08

[a] All measurements at 25 °C. [b] Key: 8-Q = 8-quinolinate; acac = acetylacetonate; PA = picolinate; DPA = 2,6-pyridinedicarboxylate acid; py = pyridine; bpy = 2,2′-bipyridine; TEA = tetraethylammonium ion. [c] Measurements made with a Gouy balance. [d] Measurements made by the Evans NMR method in Me_2SO. [e] Reference 20.

Electrolytic oxidation of the $Mn^{III}(PA)_3(H_2O)$ and $Mn^{III}(acac)_3$ complexes at low temperatures (−21 °C) in MeCN yields products with room-temperature solution magnetic moments of 3.7 and 4.1 μ_B, respectively (values close to the spin-only value for a d^3 ion). The apparent magnetic moments for both oxidized complexes decrease with time, probably as the result of decomposition and precipitation.

ESR Spectra. All of the manganese(III) complexes are ESR silent at room temperature and liquid-nitrogen temperature in both MeCN and Me_2SO, which is expected for d^4 metal ions. Exhaustive reduction of this group of complexes yields products that exhibit a six-line ESR spectrum centered at $g = 2.0$ (25 °C) that is characteristic of manganese(II) ions ($I = {}^5/_2$).

The ESR spectra at 4.1 K of the exhaustively oxidized $Mn^{III}(PA)_3(H_2O)$ and $Mn^{III}(acac)_3$ complexes exhibit an intense, broad resonance at $g = 4.0$ and a smaller signal at $g = 2.0$ in MeCN. The spectra for both of these complexes are similar to those for the $Mn^{IV}(sorbitolate)_3^{2-}$ and $Mn^{IV}TPP(N_3)_2$ complexes[23,24] in a highly anisotropic environment.

Discussion and Conclusions

The electrochemical results for this group of manganese(III) complexes, which are summarized in Figures 1 and 2 and Table I, confirm that most undergo reversible one-electron reduction and oxidation. However, at room temperature the oxidized species rapidly decompose. Within the group the $Mn^{III}(PA)_3(H_2O)$ complex exhibits the most positive redox potentials for the Mn(III)/Mn(II) and Mn(III)/Mn(IV) couples. However, the $TEA[Mn^{III}(DPA)e_2]$, $Mn^{III}(DPA)(DPAH)(EtOH)$, and $Mn^{III}(DPA)(PA)(H_2O)$ complexes have redox potentials and absorption spectra similar to those for the $Mn^{III}(PA)_3(H_2O)$ complex. The infrared spectrum for this complex includes two distinct carbonyl stretching bands (1720 and 1698 cm^{-1}) that are characteristic of the $-C(O)OH$ and $-C(O)O^-Mn^{III}$ groups, respectively. This prompts us to conclude that the coordination environment may be the same for these complexes and that the H_2O of the $Mn^{III}(PA)_3(H_2O)$ complex actually is a ligand in the form of an OH^- ion with one of the carboxylates of a PA displaced and protonated $[Mn^{III}(PA)_2(PAH)(OH)]$.

The $Mn^{III}(PA)_2(PAH)(OH)$ complex has donor groups that are consistent with those in a proteinacious environment and the redox thermodynamics that are essential for the oxidation of H_2O to O_2. Hence, it provides insight to the likely nature of the manganese centers in the multinuclear biocatalyst of photosystem

(23) Camenzind, M. J.; Hollander, F. J.; Hill, C. L. *Inorg. Chem.* **1983**, *22*, 3776.
(24) Richens, D. T.; Sawyer, D. T. *J. Am. Chem. Soc.* **1979**, *101*, 3681.

II and can serve as a reaction mimic for the biological system.

On the basis of the electrochemical, spectroscopic, and magnetic data, a reasonable set of redox reactions can be proposed for the $Mn^{III}(PA)_2(PAH)(OH)$ complex in MeCN (similar reactions are suggested for the other complexes).

$$Mn^{III}(PA)_2(PAH)(OH) + e^- \underset{+0.71\ V}{\overset{+0.58\ V\ vs.\ NHE}{\rightleftharpoons}} Mn^{II}(PA)_3^- + H_2O \quad (1)$$

The reversible reduction of the complex is shifted to more positive potentials in the presence of protons, and the solution contains free picolinic acid.

$$Mn^{III}(PA)_2(PAH)(OH) + H^+ \xrightarrow{H_2O} Mn^{III}(PA)_2(H_2O)_2^+ + PAH \quad (2)$$

$$Mn^{III}(PA)_2(H_2O)_2^+ + e^- \xrightarrow{+0.90\ V} Mn^{II}(PA)_2(H_2O)_2 \quad (3)$$

Oxidation of the $Mn^{III}(PA)_2(PAH)(OH)$ complex is a reversible process on a time scale of seconds

$$Mn^{III}(PA)_2(PAH)(OH) \underset{+1.57\ V}{\overset{+1.64\ V}{\rightleftharpoons}} Mn^{IV}(PA)_2(PAH)(OH)^+ \quad (4)$$

but at room temperature the Mn(IV) species decomposes via oxidation of solvent or supporting electrolyte.

$$Mn^{IV}(PA)_2(PAH)(OH)^+ \xrightarrow{SH} Mn^{III}(PA)_2(H_2O)_2^+ + PAH + (1/n)[SH(OH)]_n \quad (5)$$

Although the oxidized complex is stable at −21 °C, addition of OH^- causes it to be reduced.

$$Mn^{IV}(PA)_2(PAH)(OH)^+ + OH^- \xrightarrow{SH} Mn^{III}(PA)_2(PAH)(OH) + (1/n)[SH(OH)] \quad (6)$$

Reference to the data of Table I indicates that each of the manganese(III) complexes probably has three hard bases (RO^-, OH^-, $RC(O)O^-$) and three soft bases (py-N, $R_2C(O)$, H_2O) in the first coordination sphere. Also, the 8-quinolinate (8-Q) ligand stabilizes the Mn(III) oxidation state to a much higher degree than the other ligands. The acetylacetonate ligand is intermediate between 8-quinolinate and picolinate. The limited height of the reverse peak from the voltammetric oxidation of $Mn^{III}(8\text{-}Q)_3$ (Figure 3) indicates that the $Mn^{IV}(8\text{-}Q)_3^+$ species is unstable and rapidly decomposes by intramolecular electron transfer.

$$Mn^{III}(8\text{-}Q)_3 \underset{+1.14\ V}{\overset{-e^-,\ +1.21\ V}{\rightleftharpoons}} Mn^{IV}(8\text{-}Q)_3^+ \xrightarrow{H_2O} Mn^{III}(8\text{-}Q)_2(H_2O)^+ + \text{polymer} \quad (7)$$

The mixed-ligand complex, $Mn^{III}(8\text{-}Q)_2(acac)$, is noteworthy because this combination of ligands provides the highest stabilization of the Mn(III) and Mn(IV) oxidation states, but they are the least resistant to intramolecular oxidation by Mn(IV). In contrast, the $Mn^{III}(DPA)(PA)(H_2O)$ and $Mn^{III}(DPA)(bpy)(H_2O)^+$ complexes appear to be especially good mononuclear models for the coordination environment of the manganese cofactor of photosystem II.

Water Oxidation. A guiding factor for the design of model manganese systems for the cofactor in photosystem II is that they must have sufficiently positive oxidation potentials to be viable oxidants of water. The diversity of this thermodynamic limit is outlined by the redox potential manifold for the oxidation of H_2O to O_2 (Figure 6).[25] This emphasizes that multielectron steps generally have lower potentials than one-electron steps. The one-electron oxidation of H_2O to ·OH has an exceptionally positive potential, results in a biologically hazardous species, and is not a resonable path for the oxidation of H_2O to oxygen by the

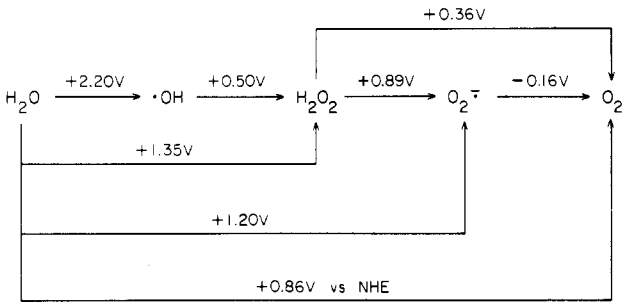

Figure 6. Redox potentials at pH 7.0 and 25 °C for the oxidation of H_2O. Potentials [V vs. NHE (−0.244 V vs. SCE)] are listed for 1e, 2e, 3e, and 4e oxidations; the standard state for all species is unit activity.

Scheme I

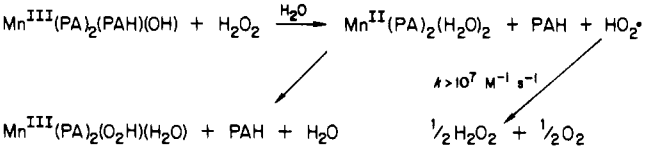

manganese cofactor of photosystem II. Even the concerted two-electron step requires an oxidizing agent with a potential of at least +1.35 V vs. NHE. Although most of the mononuclear manganese(III) complexes of Table I have sufficiently positive potentials for their III/IV couple, they are only effective as one-electron oxidants.

The results of Figure 2 indicate that the $Mn^{IV}(PA)_2(PAH)(OH)^+$ complex oxidizes OH^-. However, the redox potential is not adequate to produce free ·OH; its facile reaction with organic substrates drives the reaction to completion. For this reason, the manganese cofactor of photosystem II almost certainly contains at least two manganese ions that can act in concert and serve as a template to facilitate the formation of an O–O bond from two bound H_2O molecules (one per each metal ion).

The results of Figure 4 confirm that the $Mn^{III}(PA)(PAH)(OH)$ complex oxidizes H_2O_2 by a one-electron process (Scheme I) that is consistent with the redox thermodynamics [$E^{\circ\prime}(H_2O_2/O_2^{-}\cdot) = +0.89$ V in H_2O at pH 7 (Figure 6) and $E^{\circ\prime}[Mn(III)/Mn(II)] = +0.90$ V in MeCN (eq 3)]. The rapid disproportionation of $HO_2\cdot$ derives the reaction to completion.

However, because the conversion of H_2O to H_2O_2 in photosystem II appears to require two manganese(IV) ions, their Mn(III)/Mn(II) redox potentials only need to be more positive than +0.36 V vs. NHE (Figure 6) to bring about a concerted four-electron process.

$$[Mn^{IV}]_2 + 2H_2O \rightarrow [Mn^{II}]_2 + O_2 + 4H^+ \quad (8)$$

Such a proposition is consistent with the recent identification of a two-manganese center in the 34-kDA protein that has been isolated from chloroplasts.[10] An alternative model is a four-manganese cluster such that a concerted four-electron oxidation by four manganese(III) ions of two H_2O molecules is facilitated.

$$[Mn^{III}]_4 + 2H_2O \rightarrow [Mn^{II}]_4 + O_2 + 4H^+ \quad (9)$$

Such a system would need to have coordination environments about the manganese(III) centers to result in Mn(III)/Mn(II) redox potentials of at least +0.86 V vs. NHE (Figure 6). The mononuclear systems of Table I are far short of this limit, but the $Mn^{III}(PA)_2(H_2O)_2^+$ complex represents a configuration with a redox potential of about +0.9 V vs. NHE.

Both two-manganese and four-manganese models that are based on the complexes of Table I are under study. The goal is to achieve a system that will efficiently oxidize water to H_2O_2 and O_2. The picolinic acid, 8-quinolinol, and bipyridine ligands provide donor groups that are similar to the biological ligands provided by aspartic acid, glutamic acid, histidine, and tyrosine.

Acknowledgment. This work was supported by the National Institutes of Health under Grant No. GM-22761.

(25) Sawyer, D. T.; Nanni, E. J., Jr.; Roberts, J. L., Jr. *Adv. Chem. Ser.* **1982**, *No. 201*, 585.